Journal of Materials Chemistry B

Accepted Manuscript

ROYAL SOCIETY OF CHEMISTRY

www.rsc.org/materialsB

Journal of Materials Chemistry B

ARTICLE

Metabolizable dopamine-coated gold nanoparticles aggregates: Preparation, characteristics, computed tomography imaging, acute toxicity, and metabolism *in vivo*

Received 00th January 20xx,
Accepted 00th January 20xx

DOI: 10.1039/x0xx00000x

www.rsc.org/

Yao Yu, Youshen Wu, Jiajun Liu, Ke Li, Daocheng Wu*

To improve the computed tomography (CT) imaging ability and toxicity of gold nanoparticles (AuNPs), hydrophilic dopamine (DPA)-coated gold nanoparticles (AuNPs) (MSA AuNPs@DPA) aggregates (42 ± 2.65 nm) were obtained by assembling MSA AuNPs@DPA (5-6nm) with the use of polyethyleneimine (PEI). They were rapidly degraded into MSA AuNPs@DPA with PEI in the blood. The acute toxicity test showed that the maximum tolerated doses of MSA AuNPs@DPA and MSA AuNPs@DPA aggregates were larger than 4.8 and 4.6 g kg^{-1}, respectively, which are much higher doses than those of the commonly used citric acid-stabilized AuNPs (CA AuNPs) (2.97 g kg^{-1}). The metabolism test *in vivo* showed the elimination rates of MSA AuNPs@DPA aggregates and MSA AuNPs@DPA were 0.848 and 0.955, respectively. Most of the aggregates were eliminated by the kidney after 5 days and excreted by urine, whereas CA AuNPs remained *in vivo* and were concentrated in some organs. The $t_{0.5}$ values of MSA AuNPs@DPA and MSA AuNPs@DPA aggregates were 24.28 and 43.68 h, respectively, meaning that MSA AuNPs@DPA aggregates had a much longer circulation time. Similarly, the CT absorption value of MSA AuNPs@DPA aggregates was much higher than that of the commonly used nonionic iodinated CT contrast agent iohexol and CA AuNPs at the same concentration. Thus, MSA AuNPs@DPA aggregates possess characteristics such as ease of fabrication, long circulation time, hypotoxicity, and excellent CT absorption value, which suggests their great potential applications *in vivo*.

Introduction

Gold nanoparticles (AuNPs) with certain physical, chemical, and biological properties have recently attracted considerable attention[1]. Owing to their stability in solutions and inertness *in vivo*, AuNPs have been extensively used in biomedical fields, such as drug delivery, disease detection, diagnosis, and photothermal therapy[2,3]. In particular, AuNPs are used as computed tomography (CT) contrast agents because of their excellent characteristics of high CT absorption ability, tunable sizes, and controllable surfaces[4,5]. As a commonly used nonionic iodinated commercial small-molecule CT contrast agent with three iodine atoms, iohexol has a high CT absorption value *in vivo* but exhibits short circulation time and definite renal toxicity, thereby limiting its extensive application; and AuNPs has 2.7-fold higher CT absorption value than that of iohexol and their derivatives[6]. Theoretically, higher Au concentrations can enhance CT absorption value *in vivo*, however, AuNPs aggregation occurs, and large-scale production of AuNPs with high Au concentrations under mild conditions is difficult. AuNPs aggregation seriously impedes injection, thereby causing toxicity *in vivo*. Assembling ultrasmall AuNPs into large aggregates may be an effective technique to facilitate their enrichment if they could be divided or degraded into ultrasmall AuNPs *in vivo* and make large-scale production possible under wild condition. In addition, organic polymer coatings on the surface of AuNPs not only hinder AuNPs from aggregating but also enhance their biocompatibility and stability[7]. Kim *et al.* reported that polyethylene glycol (PEG)-coated AuNPs with a particle size of 30 nm possessed a CT absorption value 5.7 times higher than that of currently available iodine-based CT contrast agents[7]. PEG-coated AuNPs could be stable and monodispersed at a high concentration of 140 mg mL^{-1} and may impart antibiofouling properties, which prolong their circulation time *in vivo*. However, the main obstacle to the use of AuNPs and their improved formulations as CT contrast agents in clinical practice is their toxicity. So far, their metabolism pathways *in vivo* have been unclear and controversial[8,9]. Some studies have shown that AuNPs are uptaken by human cells but do not

[a] *Key Laboratory of Biomedical Information Engineering of Ministry of Education, School of Life Science and Technology, Xi'an Jiaotong University, Xi'an 710049, China. E-mail: wudaocheng@mail.xjtu.edu.cn*

† Electronic Supplementary Information (ESI) available. See
DOI: 10.1039/x0xx00000x

Journal of Materials Chemistry B

ARTICLE

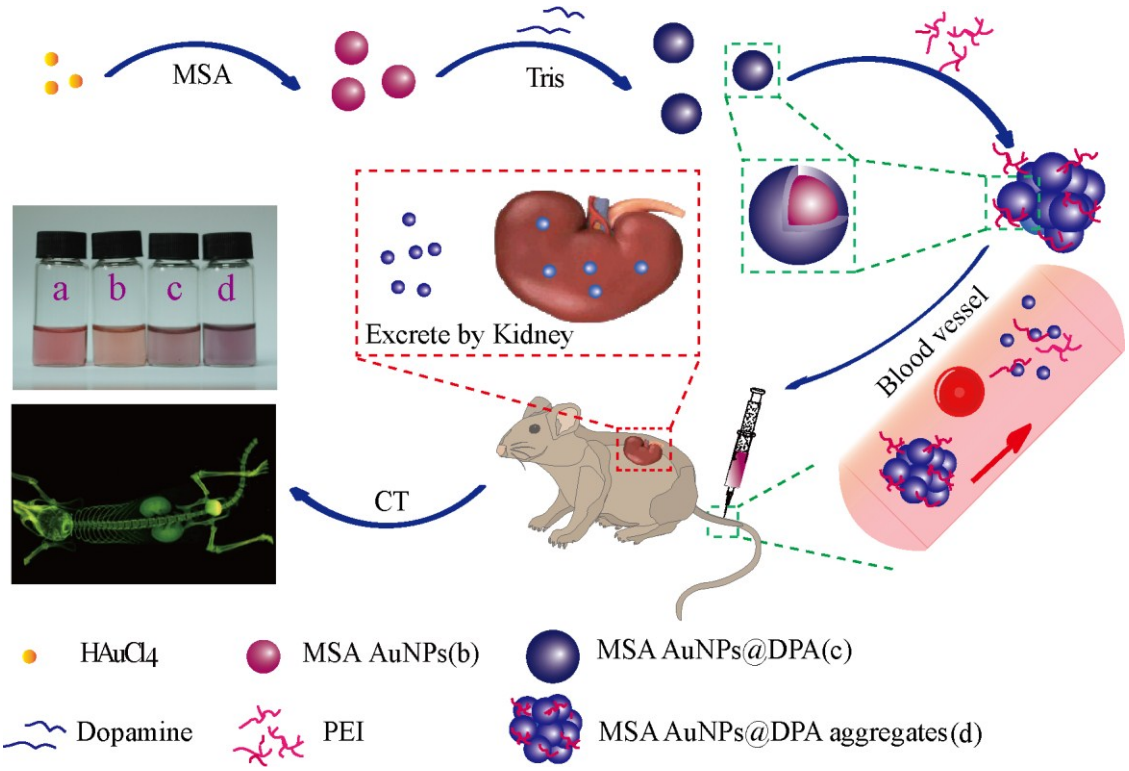

Scheme 1 Schematic represent the synthetic process, application in CT imaging and metabolic pathways *in vivo* of MSA AuNPs@DPA aggregates. The character a,b,c,d represented the CA AuNPs, MSA AuNPs, MSA AuNPs@DPA and MSA AuNPs@DPA aggregates respectively.

cause acute toxicity[3,10]. On the contrary, Leong *et al.* [11] reported the toxicity of AuNPs by their LD_{50} value, which was 750 mg mL^{-1}. Similarly, damaged organ pathological sections were found in mice after they were intravenously injected with AuNPs[12]. In 2015, ultrasmall AuNPs that consist of Au cores and organic shells show a bactericidal effect at low concentrations, indicating their toxicity to microorganisms[13]. Notably, the majority of AuNPs are enriched in reticuloendothelial system-rich organs, such as liver and spleen[14]. AuNPs accumulation in these organs results in adverse effects and may be the reason for the toxicity of AuNPs. In addition, Xu *et al.* showed that different sizes of AuNPs provide varying X-ray absorption coefficients; larger AuNPs size within the range of 4 nm to 60 nm lead to smaller X-ray absorptions[15]. Moreover, Thompson *et al.* reported that AuNPs smaller than 1.4 nm can induce cytotoxicity[9], and other nanoparticles smaller than 8 nm are excreted by the kidney[16]. Thus, AuNPs 1.4 nm to 8 nm in size might not be concentrated in organisms in the long run and could probably be used as contrast agents for CT imaging. However, Kreyling *et al.* reported that polymer-coated AuNPs with a size of 4.8 ± 0.9 nm were concentrated in the liver and spleen based on inductively coupled plasma-mass spectrometry results[17]. Thus, 1.4 nm to 8 nm AuNPs could be discharged by the kidney only if they have antifouling surfaces. More recently, a company called Nanoprobes synthesized low-toxicity 1.9 nm AuNPs with highly water-soluble organic shells; compared with iohexol, the fabricated AuNPs showed significant CT imaging enhancement and, more importantly, were cleared by the kidney *in vivo*. However, according to product instructions, these expensive AuNPs, with an unclear chemical composition, demonstrated a short circulation time (approximately 4 h), and the percentage of injected dose per gram blood was lower than 10% in 30 min, which does not match the reported circulation time[18]. The kidney metabolism pathway of AuNPs may be best verified by a urinary excretion study, and more convincing results, such as pathological sections, should be provided to show the clearance of AuNPs by the kidney. Unfortunately, to date, few reports on this topic are available in the literature. Most studies on AuNPs and their related carriers as CT contrast

agents focused on their CT imaging properties and the relationship of these properties with the physical characteristics of AuNPs; nevertheless, some of these characteristics are associated with toxicity.

Dopamine (DPA), a mussel-inspired adhesive molecule, has recently become popular as an excellent coating material for drug carriers because of its water solubility and biocompatibility, which can transform hydrophobic surfaces of materials into hydrophilic[19,20]. Liu *et al.* coated AuNPs with DPA, and the DPA-coated AuNPs did not show notable histological toxicity to the liver of mice and were stable *in vivo* for more than six weeks. Although DPA coating can significantly improve some properties of AuNPs, most AuNPs are still enriched in the liver and are not excreted for a long time due to the big size.

With the aforementioned findings from different studies as bases, we conclude that if AuNPs range from 1.4 nm to 8 nm in size are coated with DPA and then fabricated into aggregates with a suitable conjugation reagent in such a way that their rapid degradation in the blood is ensured, not only the improvement of the water solubility and metabolizable character in vivo of such AuNPs but also produces on a large scale with high Au concentrations under mild conditions. Thus, we developed a novel protocol to prepare polyethyleneimine (PEI)-assembled DPA-coated AuNPs (MSA AuNPs@DPA aggregates) (Scheme 1). First, 4 nm to 5 nm ultrasmall AuNPs (MSA AuNPs) were synthesized using 2-mercaptosuccinic acid (MSA) and sodium borohydride ($NaBH_4$) as the stabilizing and reducing agents, respectively. Then, MSA AuNPs@DPA were obtained by coating MSA AuNPs with approximately 1 nm of DPA layer. Finally, MSA AuNPs@DPA were assembled by electrostatic interaction with the use of the proper ratio of PEI because the positively charged PEI can be conjugated with the negatively charged MSA AuNPs@DPA. MSA AuNPs@DPA aggregates can be rapidly degraded into MSA AuNPs@DPA in the blood. MSA AuNPs@DPA aggregates not only showed superior CT absorption values and prolonged retention time *in vivo* but also significantly reduced the difficulties involved in concentrating AuNPs. Consequently, large-scale production of these aggregates are cost effective and feasible. More importantly, even high-dosage MSA AuNPs@DPA aggregates were cleared by the kidney, which implies that the aggregates would not be concentrated in the body and could cause only very low toxicity. Therefore, MSA AuNPs@DPA aggregates are expected to be one of the most promising CT contrast agents in the future.

Experimental

Chemicals

Hydrogen tetrachloroaurate trihydrate ($HAuCl_4 \cdot 3H_2O$), DPA, and MSA were purchased from Sinopharm Chemical Reagent Co., Ltd. (Shanghai, China). Sodium citrate, $NaBH_4$, tris (hydroxymethyl) aminomethane (Tris), phenobarbital, sodium carbonate (Na_2CO_3), KBr, and phosphate-buffered saline (PBS), and PEI (M.W. 600) were purchased from Aladdin Chemistry Co., Ltd. (Shanghai, China). 3-(4, 5-Dimethyl-2-thiazolyl)-2, 5-diphenyl- tetrazolium bromide (MTT) and dimethyl sulfoxide (DMSO) were obtained from Sigma (St. Louis, USA). All reagents were of analytical grade and used without further purification. Double-distilled water was used throughout this study.

Cells and animals

Fibroblasts and Hepa cell lines were purchased from the School of Life Science and Technology, Xi'an Jiaotong University, China. PRMI-1640 medium, high-glucose medium, fetal bovine serum (FBS), penicillin, and streptomycin were obtained from Thermo Fisher Scientific Inc. (MA, USA).

BALB/c mice were purchased from the School of Medicine, Xi'an Jiaotong University. The mice (weighing approximately 25 g) were kept under standard housing conditions. The animal experiments were approved by the Ethics Committee of Xi'an Jiaotong University.

Preparation of MSA AuNPs, MSA AuNPs@DPA, and MSA AuNPs@DPA aggregates

We employed MSA as the stabilizing agent and $NaBH_4$ as the reducing agent to produce 4–5 nm AuNPs (MSA AuNPs). Briefly, 0.5 mL of 1 wt% $HAuCl_4 \cdot 3H_2O$, 0.5 mL of 0.1 mol L^{-1} Na_2CO_3, and 0.025 mg of MSA were mixed uniformly into a 50 mL volumetric flask. Double-distilled water was used to metered volume and transferred into an acid-cleaned conical flask. After a few minutes in ice-water bath, 2.5 mL of 0.5 mg mL^{-1} $NaBH_4$ solution was added into the flask. After strenuous stirring for 15 min, MSA AuNPs were obtained.

MSA AuNPs@DPA were prepared as follows: 9.9 mL of 100 mmol L^{-1} Tris and 0.1 mL of 1 mg mL^{-1} DPA solution were mixed uniformly in a cleaned conical flask. Then, 10 mL of MSA AuNPs was added, and the mixture was stirred slowly for 3–4 h at room temperature. The obtained MSA AuNPs@DPA were concen-trated by centrifugation at 11000 rpm for 30 min and repeated thrice.

MSA AuNPs@DPA aggregates were prepared by electrostatic interaction of the positively charged PEI and negatively charged MSA AuNPs@DPA. Briefly, 70 µL of 0.078 mg mL^{-1} PEI solution was added into 5 mL of the prepared MSA AuNPs@DPA solution with an Au atom concentration of 0.0233 mg mL^{-1} and then stirred for 1 h. The final MSA AuNPs@DPA aggregates were obtained by centrifugation at 10000 rpm for 30 min. To investigate the influence of PEI concentrations to the aggregates, we varied PEI concentration from 0.078 mg mL^{-1} to 0.5 mg mL^{-1}, and their sizes were measured with a Malvern instrument (Malvern, UK).

Commonly used citric acid-stabilized AuNPs (CA AuNPs), which were obtained following the method reported by Kimling *et al.* [21], served as the control group.

Characterizations

Transmission electron microscopy (TEM) measurements

The morphology and composition of the prepared MSA AuNPs, MSA AuNPs@DPA, and MSA AuNPs@DPA aggregates were analyzed by transmission electron microscopy (TEM) (JEOL JEM-100SX) and high-resolution TEM (JEOL JEM-2100F, Japan), respectively. For TEM analysis, the samples in aqueous solution were dropped into a carbon-coated ultrathin copper grid and measured with a 75 kV electron source for TEM observation, the high-resolution TEM was measured with a 200 kV electron source. The size distribution histogram data were processed using Origin 9.0.

UV/Vis spectra, Fourier transform infrared analysis, and stability test

Ultraviolet/visible (UV/Vis) measurements were performed with a T90 UV/Vis spectrophotometer (PG Instrument Ltd., China). Samples were placed into suitable cells, and spectral wavelength was scanned from 400 nm to 700 nm.

The Fourier transform infrared (FTIR) spectra of the samples were recorded with Bruker Optics Tensor 27 spectrometer (Ettlingen, Germany). KBr was used and mixed with sample powders to make tablets for measurements.

The stabilities of the samples were measured using UV/Vis spectra and a Malvern instrument. The maximum absorbance peaks of the samples were measured at regular time points. The changes in the colors of the samples in PBS solution with high ionic strength were observed. The zeta potential data and the hydraulic radii of the samples were obtained at regular times with a Malvern instrument. Exactly 0.8 mL of sample was placed into a suitable vessel at room temperature, and the size distribution, zeta potential, and maximum absorbance peaks of each sample were examined intervals for 3 months.

Degradation of MSA AuNPs@DPA aggregates in the blood

To observe the degradation of MSA AuNPs@DPA aggregates in the blood, we mixed the prepared MSA AuNPs@DPA aggregates with the FBS and buffer solutions with different pH values, i.e., from 4 to 10. Exactly 100 µL of MSA AuNPs@DPA aggregates was mixed with 900 µL of blood serum and buffer solutions. The ratio of the aggregates was similar to that of the aggregate solution in the blood by intravenous injection. A Malvern instrument was used to measure the sizes and zeta potentials of the mixed solutions at different times.

X-ray-based CT imaging

To evaluate the CT contrast efficiencies of the aforementioned samples and compare them with those of iohexol and CA AuNPs, we dispersed the samples in water at similar concentrations and measured their CT absorption values by CT scanning using CT series 5000 apogee tube (Oxford Instrument, USA). The CT imaging parameters were as follows: tube voltage, 50 kVp; tube current, 1 mA; spot size, 35 µm; and resolution ratio, 1944/3072.

For *in vivo* CT imaging, 200 µL each of MSA AuNPs@DPA (200 mg Au kg^{-1} body weight), MSA AuNPs@DPA aggregates, CA AuNPs, and iohexol was intravenously injected into the mice. The mice were then anesthetized with 100 µL of 2 wt% phenobarbital by intraperitoneal injection. The CT images at different times were detected by CT scanning. *In vivo* CT absorption values of the samples at different times in various organs were measured and calculated by MATLAB after data reconstruction.

Cell culture and cytotoxicity assay

Fibroblasts and Hepa cell lines were cultured in high-glucose and PRMI-1640 media supplemented with 40 µg mL^{-1} streptomycin sulfate, 50 µg mL^{-1} penicillin, and 10% of FBS in a humidified incubator (Sanyo, Japan) at 37 °C and 5% of CO_2 condition. Cells were harvested and re-suspended in fresh media before plating.

Cytotoxicity was measured by MTT assay. Fibroblasts and Hepa cells were seeded into a 96-well plate, subsequently incubated for 24 h, and then incubated with different concentrations of MSA AuNPs, MSA AuNPs@DPA, and MSA AuNPs@DPA aggregates for another 24 h. The fibroblasts and Hepa cells were rinsed with PBS and incubated with MTT solution (10 µL, 0.5 mg mL^{-1}) in a suitable medium for 4 h at 37 °C. Afterward, the medium was discarded, and the generated formazan was dissolved with DMSO. The absorbance was measured using Thermo Scientific Multiskan GO microplate spectrophotometer (New York, USA) at 490 nm. The experiments were repeated five times, and the data were analyzed by using GraphPad Prism 5.

Haemolytic assay was also completed following standard method to prove the safety for blood cells. More details can be seen in the supporting information.

Acute toxicity

To determine the acute toxicities of the samples, 48 of the BALB/c mice, half of which are male and the other half female, were randomly divided into four groups: 1) blank group, 2) MSA AuNPs@DPA group, 3) MSA AuNPs@DPA aggregate group, and 4) CA AuNPs group (control). The mice were intravenously injected with the maximum dosage (200 µL) of the aforementioned samples. The maximum tolerated dose (MTD) was used to evaluate acute toxicity. MTD refers to the highest dose of a pharmacological treatment that will produce the desired effect without unacceptable toxicity. Injections were administered once every 2 days until a mouse died. If the mice were alive after 15 days, then the experiments were stopped, and the mice were weighed at the end of the tests. To study the damage in the organs, the mice organs from each group were collected and fixed in 4% paraformaldehyde solution for preparation of pathological sections in 1 day. These organs were then cut into 5 mm^3 sections, stained with hematoxyline and eosin, and evaluated using a microscope (Nikon, Japan). To observe the distribution of AuNPs in the liver, the livers from the different groups were collected and initially fixed in 2.5% glutaraldehyde (pH 7.0, 0.1 mol L^{-1} PBS), and then fixed with 0.01 perosmic oxide for 2 h at 4 °C. The samples were dehydrated in an alcohol series after being rinsed with water, embedded, cut into little dice smaller than

1 mm^3, and then observed using JEOL JEM-100SX after slicing on a microtome.

Metabolism *in vivo*

To analyze the metabolism pathways of MSA AuNPs@DPA, MSA AuNPs@DPA aggregates, and CA AuNPs *in vivo*, 40 BALB/c mice, half of which are male and the other half female, were randomly divided into four groups: 1) blank group, 2) MSA AuNPs@DPA group, 3) MSA AuNPs@DPA aggregate group, and 4) CA AuNPs group (control). The mice were intravenously injected with the aforementioned samples with similar concentrations of 200 mg kg^{-1} body weight. Approximately 3 mL of mice urine was obtained using metabolic cages each day and continued for 5 days. Inductively coupled plasma-emission spectroscopy (ICP-AES; Shimadzu ICPE-9000, Japan) was used to quantitatively measure the Au concentrations in the urine samples. Finally, with the ICP results, the metabolism dynamics of these samples were calculated using DAS 2.0 and WinNonlin software.

Statistical analysis

Data are shown as means ± standard deviations of independent experiments. One-way ANOVA was performed to determine the differences among the samples. *P* values smaller than 0.05 were considered statistically significant.

Results and discussion

Preparation and characterization of MSA AuNPs@DPA aggregates

AuNPs have recently become attractive reagents in biomedical applications. The common method for synthesizing uniform hydrophilic Au particles is the Turkevich–Frens citrate reduction route and its variations[22]. The most common route for the synthesis of ultrasmall AuNPs less than 10 nm is employing borohydride to reduce Au salts in the presence of a mercapto group that contains a capping agent in either a two-phase liquid/liquid system or an organic solvent[23]. A very hydrophilic molecule with a thiol group is needed to obtain ultrasmall AuNPs in water. Scientists have used thioether-terminated polymer[24] and dimercaptosuccinic acid[25] as stabilizing agents to obtain ultrasmall AuNPs 1 nm to 4 nm in size and subnanometer Au aggregates in water. The relatively small molecular weight of a thiol stabilizer ensures the proportion of Au atom per mole molecule. Moreover, Niu *et al.* reported the synthesis of AuNPs in the 30–150 nm size range with MSA as the reducing agent by tuning the ratio of MSA and Au ions [26].

Drawing from the aforementioned studies, we assumed that MSA with a thiol group was used as the stabilizing agent and employed another strong reducing agent, $NaBH_4$. Thus, the reducing and stabilizing procedures were separately performed. The nucleation and growth rates of AuNPs were controlled by adjusting the proportion of Au salts, reducing agents, and MSA in the preparation process. Thus, differently sized AuNPs were obtained. MSA is a water-soluble molecule

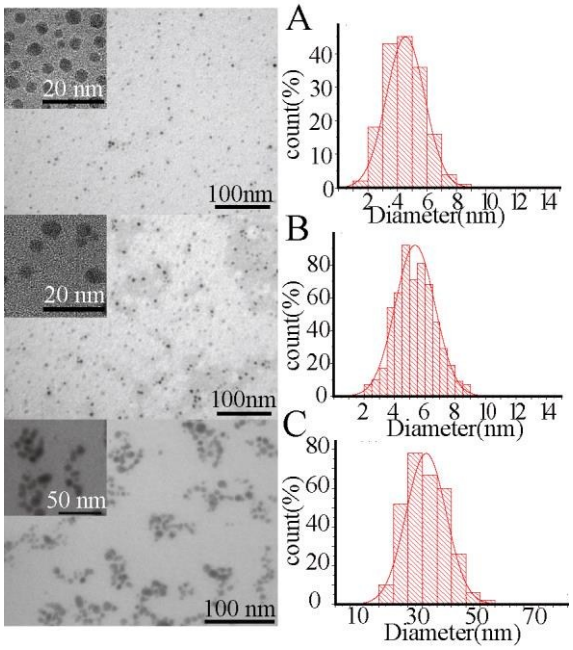

Fig. 1 The TEM and high resolution TEM imaging and size distribution histogram of MSA AuNPs, MSA AuNPs@DPA and MSA AuNPs@DPA aggregates.

with two carboxyl groups, the analog of which is malic acid, an active molecule in Krebs cycle with excellent biocompatibility. MSA was coated on the surface of the newly formed Au seeds once the reducing agent $NaBH_4$ was added. Consequently, the favorable water solubility of the MSA molecules on the surface prevented the MSA-coated Au seeds from growing. The low temperature of the ice bath limited the reducing speed of the Au ions, thereby facilitating the coating and stabilization processes. The stabilization and reducing processes were controlled by regulating the ratio of MSA and $NaBH_4$ to obtain AuNPs with sizes that range from 4 nm to 5 nm. The ratio of MSA and Au ions was changed for many times and the measurement data was shown in Fig. S1. Specific size of AuNPs could be obtained by regulating the ratio of the MSA and Au ions.

Bare AuNPs are not stable enough for further use in medical application. A shell with good biocompatibility and stability can significantly improve the properties of AuNPs. DPA has become a novel coating material because of its excellent biocompatibility, biodegradability, and antifouling properties, which made this compound easy to coat on almost all materials with tunable thickness and permanent stability under mild polymerization conditions[20]. Therefore, we coated MSA AuNPs with DPA to improve their stability and biocompatibility. In addition, to enhance the *in vivo* CT imaging of AuNPs and easily produce an Au solution of a higher concentration, we used PEI to assemble the MSA AuNPs@DPA by electrostatic interaction. The interaction made the assembled AuNPs irregularly shaped with narrow size distribution, stable, and easy to concentrate when PEI was with a proper concentration, which makes its large-scale production feasible. When the concentration of PEI increased threefold, AuNPs@DPA aggregated immediately. MSA

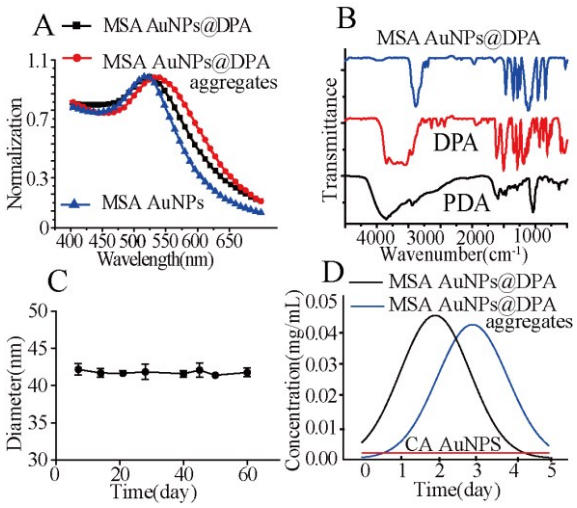

Fig. 2 (A) The UV/Vis spectra of MSA AuNPs, MSA AuNPs@DPA and MSA AuNPs@DPA aggregates;(B) the FTIR spectra of MSA AuNPs@DPA, dopamine (DPA) and polydopamine (PDA) ;(C) The stability of MSA AuNPs@DPA aggregates particle in 2 months;(D) The gold concentration in urine after different days by injection of MSA AuNPs, MSA AuNPs@DPA and MSA AuNPs@DPA aggregates *in vein* at the same concentration.

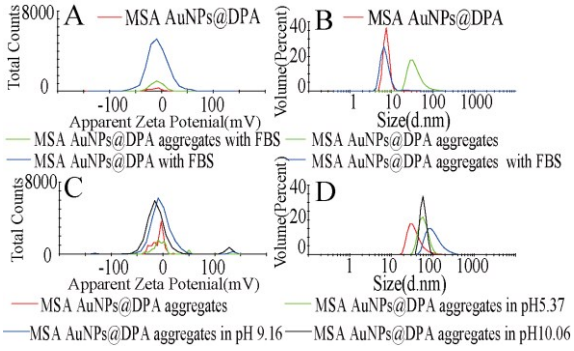

Fig. 3 The Zeta potential data (A, C) and size distribution data (B,D) of MSA AuNPs, MSA AuNPs@DPA aggregates with FBS and FBS (A,B), MSA AuNPs@DPA aggregates in buffer with different pH (C,D).

AuNPs@DPA were concentrated twice by centrifugation at 10000 rpm for 30 min. By contrast, MSA AuNPs@DPA aggregates were enriched by 10 times through the same process. Thus, the process demonstrated a much higher efficiency in enriching MSA AuNPs@DPA aggregates at higher concentrations than in enriching MSA AuNPs@DPA. TEM images showed that MSA AuNPs and MSA AuNPs@DPA have relatively uniform spherical shapes and narrow size distributions with mean diameters of 4.5 ± 1.07 and 5.4 ± 1.27 nm, respectively, whereas MSA AuNPs@DPA aggregates have a mean diameter of 42 ± 2.65 nm with uniform size and irregular shape (Fig. 1). High-resolution TEM images revealed the crystalline nanostructure of MSA AuNPs and the clear core-shell structure of the MSA AuNPs@DPA with DPA coating of less than 1 nm (Fig. 1A and B insert). Fig. S2A shows that the corresponding sizes of the MSA AuNPs, MSA AuNPs@DPA, and MSA AuNPs@DPA aggregates were 4.9, 6.0, and 44 nm, respectively, which were slightly larger than those of the TEM results because of their hydration in the solution.

Fig. 2A illustrates the UV/Vis absorption peaks of the aforementioned AuNPs. The typical absorption of MSA AuNPs was at 517 nm, whereas the absorption peaks of MSA AuNPs@DPA and MSA AuNPs@DPA aggregates were at 524 and 532 nm, respectively. The slight red shift of the absorption spectrum of MSA AuNPs@DPA was due to the increased refractive index around the MSA AuNPs after DPA coating. The red shift of the MSA AuNPs@DPA aggregate absorption spectrum was due to the change in particle size, i.e., a large size led to long-wavelength absorption peak[27]. The MSA AuNPs appeared in watermelon red, whereas the MSA AuNPs@DPA aggregates appeared in purple (Scheme 1). Fig. S2B presents the images of the samples mixed with PBS. Bare MSA AuNPs in PBS turned purple or blue from watermelon red in seconds. By contrast, MSA AuNPs@DPA and MSA AuNPs@DPA aggregates maintained their colors in PBS. These results imply that bare MSA AuNPs were not as stable as MSA AuNPs@DPA and MSA AuNPs@DPA aggregates under a high ionic condition. After being stored for 3 months at room temperature, MSA AuNPs@DPA aggregates demonstrated only slight changes in size (Fig. 2C).

Fig. 2B illustrates the FTIR spectra of MSA AuNPs@DPA, DPA, and polydopamine. The peak at approximately 3400 cm^{-1} in each spectrum represents the stretching vibration of –NH. The phenolic hydroxyl group characteristic peak appeared at approximately 3147 cm^{-1}, and the peak at 1646 cm^{-1} showed the bending vibration of benzene rings. The typical functional group of C=O in polydopamine had significant absorption at 1300 cm^{-1}, implying that the characteristic peaks of DPA did not change after being coated on MSA AuNPs. This finding proved the successful coating of DPA on the MSA AuNPs surfaces.

Degradation of MSA AuNPs@DPA aggregates in the blood

The size data in Fig. 3A and B showed the size and Zeta potential data of MSA AuNPs@DPA aggregates after being mixed with the FBS. The aggregates were found to have been divided into small particles in the FBS. The degraded small particles were as large as MSA AuNPs@DPA. The zeta potential of MSA AuNPs@DPA and MSA AuNPs@DPA aggregates showed minimal difference. Such minimal difference might be because PEI molecules were still conjugated on the surface of the divided MSA AuNPs@DPA after aggregate degradation. Although MSA AuNPs@DPA aggregates were divided into MSA AuNPs@DPA once mixed with FBS, the degraded small particles were only stable in a solution within the pH range of 7.2–7.6; thus, they can be kept stable in the blood *in vivo* because the pH value of the blood is approximately 7.2–7.4. In other pH ranges, except for 7.2–7.6, the degraded small particles can aggregate into larger particles (Fig. 3C and D). In contrast, MSA AuNPs@DPA can be stable in pH values from 4 to 10. Thus, after intravenous injection, MSA AuNPs@DPA aggregates first divided into MSA AuNPs@DPA with PEI once mixed with fresh blood and were enriched in the bladder because the pH value changed to the range of 7.3–8.5. The results indicate that MSA AuNPs@DPA aggregates, unlike MSA AuNPs@DPA, can be maintained for a longer time *in vivo*

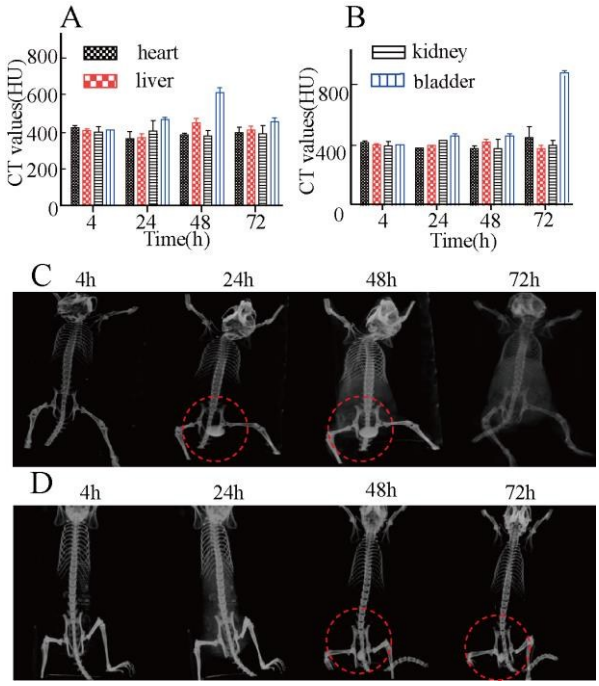

Fig. 4 The CT absorption values of different organs from the mice injected with 200 mg Kg^{-1} body weight of MSA AuNPs@DPA (A C) and MSA AuNPs@DPA aggregates (B D) in different times (the red circle labelled the bladder of the mice).

because MSA AuNPs@DPA aggregates become larger particles that need more time to be excreted by the kidney.

X-ray-based CT imaging

To facilitate the differentiation of soft tissues by CT imaging, we used contrast agents that contain high-atomic-number elements to absorb X-ray. Available CT contrast agents are mostly made of iodinate molecules and related AuNPs. Clinical contrast agents often use Omnipaque (iohexol), which is a nonionic small molecule with short circulation time and definite renal toxicity in a large dosage. Similarly, AuNPs that provided higher CT absorption values per unit weight than iodine-containing compounds have become potential CT contrast agents. Coating the hydrophilic surfaces of AuNPs with a good biocompatible material is useful to make AuNPs more efficient for CT imaging[7]. Kim *et al.* reported that PEG-coated AuNPs as CT contrast agent with a particle size of 30 nm demonstrated a relatively longer blood circulation time (4 h) and accumulated in the phagocytic cell-rich organs, such as the spleen and the liver. The CT absorption value of the agents, which concentrated in organs, increased by 40 HU for the liver and 90 HU for the spleen in 24 h at 233 mg Au kg^{-1} body weight. The AuNPs enriched in the liver and the spleen can harm the organs in the long run. Compared with common AuNPs, the MSA AuNPs@DPA and MSA AuNPs@DPA aggregates in this study showed much improved characteristics. Smaller dosages of 200 mg Au kg^{-1} body weight of the prepared MSA AuNPs@DPA and MSA AuNPs@DPA aggregates are required for CT imaging and demonstrated much better imaging effects.

Figs. 4 and 5 display the CT images and CT absorption values of the different organs (heart, liver, kidney, and bladder) before and after intravenous injection of MSA AuNPs@DPA, MSA AuNPs@DPA aggregates, CA AuNPs, and iohexol solution in different time periods. After 1 day of injection, most MSA AuNPs@DPA accumulated in the bladder, which increased the brightness of the bladder and made it significantly brighter than the other organs (Fig. 4A and C). The mice injected with MSA AuNPs@DPA aggregates (Fig. 4B and D) showed a much brighter bladder after 2 days, which was later than when MSA AuNPs@DPA was injected. However, 60 min after injection of iohexol (Fig. 5B and D), the bladder and kidney of the mice were much brighter than the other organs, revealing that iohexol was cleared through the kidney and maintained a very short circulation time *in vivo*. MSA AuNPs@DPA and MSA AuNPs@DPA aggregates demonstrated much longer circulation times (>24 and > 48 h, respectively) compared with the circulation times of iohexol (shorter than 10 min) and PEG-coated AuNPs (4 h). These phenomena might be due to the reaggregation of MSA AuNPs@DPA with PEI in the bladder, as previously described. The circulation time of the prepared MSA AuNPs@DPA aggregates was about 100 times longer than that of 1.9 nm AuNPs from Nanoprobes and 10 times as that of PEG-coated AuNPs[10]. Compared with the 1.9 nm AuNPs from Nanoprobes, MSA AuNPs@DPA aggregates were effective at a relatively low dosage and showed a much longer circulation time. Meanwhile, the CT absorption values in the liver and the spleen showed a slight change in 5 days in the MSA AuNPs@DPA group, the MSA AuNPs@DPA aggregate group, and the iohexol group, which suggests that MSA AuNPs@DPA aggregates, as well as MSA AuNPs@DPA and iohexol, were not concentrated in the liver and the spleen. By contrast, the mice injected with CA AuNPs (Fig. 5A and C) showed a brighter liver and spleen in 24 h, which indicates that the CA AuNPs accumulated in the liver and spleen in 1 day.

Based on the results of the above degradation test, MSA AuNPs@DPA aggregates can be degraded into MSA AuNPs@DPA with PEI once the aggregates mix with the blood; as a result, the metabolism pathways of the MSA AuNPs@DPA aggregates and MSA AuNPs@DPA were the same. When the MSA AuNPs@DPA with PEI enriched in the bladder, a higher concentration of PEI increased the tendency of MSA AuNPs@DPA with PEI to aggregate. In addition, considering that the pH value of urine is about 7.3–8.5, MSA AuNPs@DPA with PEI tended to gather again, which resulted in increasing time to be excreted by the kidney. Consequently, these two steps would cost more time and would cause the MSA AuNPs@DPA aggregates to have a circulation time that is longer than that of MSA AuNPs@DPA. In addition, DPA coating with good compatibility proved to serve as stealth capping similar to PEG coating[7]. Stealth coatings protect AuNPs from being uptaken in the blood, thereby resulting in long circulation times.

MSA AuNPs@DPA and their aggregates provided much higher CT absorption value (426 HU) than iohexol (362 HU) at similar elemental concentrations (Fig. 6D); thus, the former two AuNPs have longer circulation times and can be discharged by

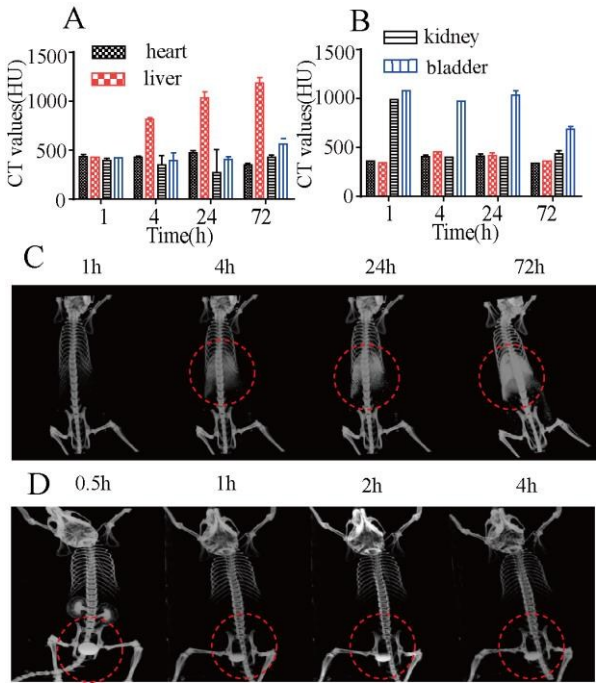

Fig. 5 The CT absorption values of different organs from the mice injected with 200 mg Kg^{-1} body weight CA AuNPs@DPA (A C) and iohexol (B D) in different times (the red circle labelled the liver in C and bladder in D of the mice).

the kidney, which makes them safe for organisms in the long run and reveals their considerable potential for CT imaging.

Cytotoxicity and acute toxicity

Fig. 6A and B show that the MSA AuNPs, MSA AuNPs@DPA, and MSA AuNPs@DPA aggregates were safe for fibroblasts and Hepa cells. MSA AuNPs@DPA and MSA AuNPs@DPA aggregates evidently had low cytotoxicity to cells and can be potentially applied *in vivo*. CA AuNPs also demonstrated low toxicity to HepG2 cells[7]. Haemolytic assay results shown in Fig. S6,it is found MSA AuNPs@DPA aggregates were safe for red

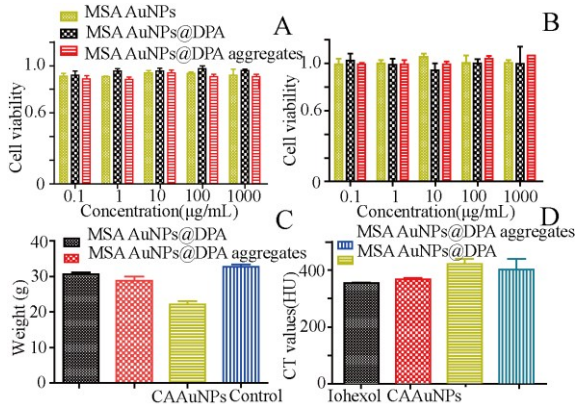

Fig. 6 (A)the cell viability of Hepa cell lines after the MTT assay, incubated with MSA AuNPs and MSA AuNPs@DPA and MSA AuNPs@DPA aggregates;(B) the cell viability of fibroblasts cell lines after the MTT assay, incubated with MSA AuNPs and MSA AuNPs@DPA and MSA AuNPs@DPA aggregates (C)The weight of mice after injecting MSA AuNPs, MSA AuNPs@DPA and MSA AuNPs@DPA aggregates every two days in 15 days;(D)The CT absorption values of iohexol, MSA AuNPs, MSA AuNPs@DPA and MSA AuNPs@DPA aggregates in heart after injecting *in vein*.

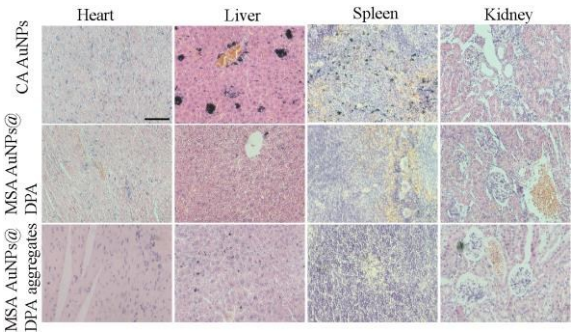

Fig. 7 The pathological sections of different organs (heart, liver, spleen, kidney) from the mice injected MSA AuNPs, MSA AuNPs@DPA and MSA AuNPs@DPA aggregates.

blood cells and neither cause hemolysis nor heamagglutination. Many studies have shown that AuNPs are safe for organisms based on cell test results. However, toxicity varies across organisms because AuNPs are enriched in organs and affected the normal abilities of the organs. Biodistribution studies have shown that most AuNPs are concentrated in some organs, such as in the liver and the spleen[28,29], which can harm organisms in the long run, especially at large concentrations. In general, CT imaging with more distinct images always owe to a large dosage of contrast agent. Abundant AuNPs injected into the blood will definitely almost instantaneously lead to adverse reactions. Therefore, a CT contrast agent should have a low viscosity at a high concentration, should not be concentrated *in vivo*, and should be excreted from the body. Nanoprobes declared that the LD_{50} value of their 1.9 nm AuNPs was 3.2 g Au kg^{-1} for BALB/c and nude mice, which is much higher than the required CT dosage. Such a large dosage, because of the viscosity and osmotic pressure, among other properties, will absolutely instantaneously lead to adverse reactions in injected animals. Moreover, in this study, LD_{50} was not employed to describe the toxicity of large-dose AuNPs. To comply with animal ethics requirements of the Ethics Committee of Xi'an Jiaotong University, we chose MTD to describe the acute toxicity of the synthesized AuNPs.

In 15 days, the mice in the CA AuNPs group died after being injected 3 times, whereas mice in the MSA AuNPs@DPA and MSA AuNPs@DPA aggregate groups were still alive. The MTD value of CA AuNPs was 2.97 g kg^{-1}, and the MTD values of MSA AuNPs@DPA and MSA AuNPs@DPA aggregates were larger than 4.8 and 4.6 g kg^{-1}, respectively. In general, LD_{50} values are far larger than MTD values. In this study, even the MTD values of MSA AuNPs@DPA and MSA AuNPs@DPA aggregates were much larger than the LD_{50} value of the 1.9 nm AuNPs, indicating that MSA AuNPs@DPA and MSA AuNPs@DPA aggregates had much lower toxicity than the CA AuNPs and the 1.9 nm AuNPs of Nanoprobes did. The difference between the MTD values of MSA AuNPs@DPA and MSA AuNPs@DPA aggregates is minimal because they have the same metabolism pathway, which was proved by CT imaging results. Both MSA AuNPs@DPA and MSA AuNPs@DPA aggregates can be discharged by the kidney and taken away by urine in a proper time. As a result, both pose minimal harm to the organs,

whereas CA AuNPs are enriched in the liver and the spleen, which leads to considerably greater toxicity.

The morphology of the typical organs, such as the heart, the liver, the spleen, and the kidney (Fig. 7), as well as the TEM images (Fig. S4) provided additional evidence to the above explanation. CA AuNPs aggregated in the liver blood capillaries, even in the thick blood vessels, in a few days, which made the liver appear to be black unlike a normal liver, which appears red. Fig. S3 shows the organ sections after CA AuNP injection at different times (on days 1 and 7); numerous black dots were found in the liver and the spleen, indicating that the amounts of CA AuNPs that accumulated in the liver and the spleen increased as administration time increased. In the MSA AuNPs@DPA and MSA AuNPs@DPA aggregate groups, almost no black dots were observed in the liver and the spleen after injection, and the kidney was inflated after injection, as shown in the pathological section. We infer that the kidney cells shrunk but did not necrotized, while the liver and the spleen were normal. The TEM images in Fig. S4 show that CA AuNPs accumulated in the liver and the spleen. CA AuNPs in the liver accumulated in the peripheral capillaries or uptaken by the cells in the liver, whereas no AuNPs were found in the livers of the mice in the other groups. The TEM images and pathological section results show that no MSA AuNPs@DPA and MSA AuNPs@DPA aggregates was found in the liver and the spleen, whereas CA AuNPs were mostly found in the blood vessels of the liver and the spleen. Therefore, MSA AuNPs@DPA and their aggregates do not concentrate in the liver and the spleen, meaning that both AuNPs have a much lower toxicity than CA AuNPs in the long run.

Furthermore, under similar feeding conditions, the weights of the mice in the CA AuNPs group evidently decreased, whereas the weights of the mice administered with MSA AuNPs@DPA and MSA AuNPs@DPA aggregates were almost equal to those of the mice in the control group (Fig. 6C). We can infer that CA AuNPs pose significant harm to the mice, whereas MSA AuNPs@DPA and their aggregates are relatively safe and suitable for future application.

Metabolism *in vivo*

Iohexol, MSA AuNPs@DPA, and MSA AuNPs@DPA aggregates *in vivo* evidently showed similar metabolism pathways. MSA AuNPs@DPA and MSA AuNPs@DPA aggregates could be excreted by the kidney and were concentrated in the bladder after 24 h and 48 h, respectively, as shown in the CT images. To study the real metabolism pathway *in vivo* of the above AuNPs, we collected urine and assessed urine drug concentration. According to the degradation test results, the aggregates divided into small AuNPs once they mixed with the blood, and the concentration of the AuNPs in the blood demonstrated a significant change in a very short time. Thus, the commonly used blood drug concentration could not represent the actual metabolism pathway of the AuNPs unlike a urine drug concentration test.

The ICP detection results showed the absence of CA AuNPs in the urine samples, which implied that AuNPs were not excreted by the kidney. These results confirmed the CT imaging results. Moreover, MSA AuNPs@DPA and MSA AuNPs@DPA aggregates showed similar metabolism curves (Fig. 2D), and the metabolic parameters are shown in Table 1. The elimination rates of MSA AuNPs@DPA and MSA AuNPs@DPA aggregates were 0.955 and 0.848, respectively, indicating that almost all these samples were eliminated by the mice, thereby leading to the low toxicity of MSA AuNPs@DPA and MSA AuNPs@DPA aggregates. These results were verified by the acute toxicity results in the previous subsection. The metabolism curves in Fig. S5 show that most MSA AuNPs@DPA aggregates can be cleared in 5 days. The $t_{0.5}$ of MSA AuNPs@DPA aggregates was 43.68 h, which was much longer than that of MSA AuNPs@DPA (24.28 h); these results agree well with the CT imaging results, thereby revealing the much longer circulation time of MSA AuNPs@DPA aggregates. These results can also be explained by the reaggregation of MSA AuNPs@DPA with PEI in the bladder, as previously described.

Parameter	Unit	MSA AuNPs@DPA aggregates	MSA AuNPs@DPA
$t_{1/2}$	h	43.678±0.251	24.284±0.551
Ke	1/h	0.029	0.062
Output rate	%	0.848	0.955
Urine output	ug	3391.6±2.564	3820±3.185
r		-0.085	-0.947

Table 1 Pharmacokinetics parameters of MSA AuNPs@DPA aggregates and MSA AuNPs@DPA.

Size and surface characteristics were evidently two factors that contributed to the metabolism pathway of MSA AuNPs@DPA aggregates. It is reported some nanoparticles smaller than 8 nm could be excreted by the kidney[16]. Thus, MSA AuNPs@DPA with a size of 5–6 nm could be cleared by the kidney, whereas CA AuNPs with a size of about 15 nm could not be cleared. MSA AuNPs@DPA aggregates were larger than 8 nm in size. However, once injected into the blood, these aggregates divided and dispersed into 5–6 nm AuNPs. Thus, MSA AuNPs@DPA aggregates and MSA AuNPs@DPA demonstrated similar metabolism pathways. With the two steps of degradation and regathering, the circulation time of MSA AuNPs@DPA aggregates was much longer, as confirmed by the CT imaging results. However, the AuNPs approximately 5 nm in size with polymer coating would be enriched in the liver and the spleen[17]; a stealth surface is important for particles to be discharged by the kidney. The DPA coating might have functioned as an antifouling surface that protected MSA AuNPs@DPA and MSA AuNPs@DPA aggregates from being uptaken. A similar phenomenon occurred in the PEG-coated AuNPs.

In summary, MSA AuNPs@DPA aggregates could divide into MSA AuNPs@DPA with PEI once they mix with the blood and then regather in the bladder because of the enrichment of PEI and the change in pH values and excreted by kidney at last. As a result, the circulation time of the aggregates was longer than

that of MSA AuNPs@DPA, but showed the same metabolism pathway with the MSA AuNPs@DPA.

Conclusions

We developed a novel method for the preparation of stable MSA AuNPs@DPA aggregates with high Au concentrations and a uniform size of 42 nm. Compared with iohexol and other AuNPs, these aggregates showed improved CT imaging results at a relatively low dosage, much lower toxicity, and much longer circulation time *in vivo*. More importantly, MSA AuNPs@DPA and their aggregates can be cleared by the kidney, indicating they could be used as promising next-generation CT contrast agents.

Acknowledgements

This work was sponsored in part by the National Basic Research Program 973 of China (No, 2011CB707903), National Natural Science Foundation of China (81228011, 81271686 and 61178085), the grants of Shaanxi province science and technology and innovation project (2011KTCL03-07) and Major industry-university-research collaboration project of Xi'an (No.CXY1423).

Notes and references

1 M.-C. Daniel and D. Astruc, *Chemical reviews*, 2004, **104**, 293-346.
2 P. Ghosh, G. Han, M. De, C. K. Kim and V. M. Rotello, *Advanced drug delivery reviews*, 2008, **60**, 1307-1315.
3 Z. Luo, K. Zheng and J. Xie, *Chemical communications*, 2014, **50**, 5143-5155.
4 R. Guo, H. Wang, C. Peng, M. Shen, L. Zheng, G. Zhang and X. Shi, *Journal of Materials Chemistry*, 2011, **21**, 5120.
5 R. Popovtze, A. Agrawal, N. A. Kotov, A. Popovtzer, J. Balter, T. E. Carey and R. Kopelman, *Nano Letters*, 2008, **8**, 4593-4596.
6 P. A. Jackson, W. N. Rahman, C. J. Wong, T. Ackerly and M. Geso, *European journal of radiology*, 2010, **75**, 104-109.
7 K. Dongkyu, S. Park, J. H. Lee, Y. Y. Jeong and S. Jon, *J. Am. Chem. Soc.*, 2007, **129**, 7661-7665.
8 N. Lewinski, V. Colvin and R. Drezek, *Small*, 2008, **4**, 26-49.
9 Y. Pan, S. Neuss, A. Leifert, M. Fischler, F. Wen, U. Simon, G. Schmid, W. Brandau and W. Jahnen-Dechent, *Small*, 2007, **3**, 1941-1949.
10 E. E. Connor, J. Mwamuka, A. Gole, C. J.Murphy and M. D. Wyatt, *Small*, 2005, **1**, 325-327.
11 A. K. Salem, P. C. Searson and K. W. Leong, *Nature Materials*, 2003, **2**, 668-671.
12 C. Lasagna-Reeves, D. Gonzalez-Romero, M. A. Barria, I. Olmedo, A. Clos, V. M. S. Ramanujam, A. Urayama, L. Vergara, M. J. Kogan and C. Soto, *Biochemical and biophysical research communications*, 2010, **393**, 649-655.
13 S. K. Boda, J. Broda, F. Schiefer, J. n. Weber-Heynemann, M. Hoss, U. Simon, B. Basu and W. Jahnen-Dechent, *Small*, 2015, DOI: 10.1002/smll.201403014.
14 W. S. Cho, M. Cho, J. Jeong, M. Choi, H. Y. Cho, B. S. Han, S. H. Kim, H. O. Kim, Y. T. Lim, B. H. Chung and J. Jeong, *Toxicology and applied pharmacology*, 2009, **236**, 16-24.
15 C. Xu, G. A. Tung and S. Sun, *Chem. Mater.*, 2008, **20**, 4167-4169.
16 A. E. Nel, L. Madler, D. Velegol, T. Xia, E. M. V. Hoek, P. Somasundaran, F. Klaessig, V. Castranova and M. Thompson, *Nature Materials*, 2009, **8**, 543-557.
17 W. G. Kreyling, A. M. Abdelmonem, Z. Ali, F. Alves, M. Geiser, N. Haberl, R. Hartmann, S. Hirn, D. J. de Aberasturi, K. Kantner, G. Khadem-Saba, J. M. Montenegro, J. Rejman, T. Rojo, I. R. de Larramendi, R. Ufartes, A. Wenk and W. J. Parak, *Nature Nanotechnology*, 2015, DOI: 10.1038/nnano.2015.111.
18 Nanoprobes, 2009. http://www.nanoprobes.com/products/AuroVist-1-9-nm Gold-X-ray-Contrast-Agent.html
19 Y. Liu, K. Ai and L. Lu, *Chemical reviews*, 2014, **114**, 5057-5115.
20 H. Lee, S. M. Dellatore, W. M. Miller and P. B. Messersmith, *Science*, 2007, **318**, 426-430.
21 J. Kimling, M. Maier, B. Okenve, V. Kotaidis, H. Ballot and A. Plech, *J. Phys. Chem. B*, 2006, **110**, 15700-15707.
22 F. G, *Nature*, 1972, 20-22.
23 M. Brust, M. Walker, D. Bethell, D. Schiffrin and R. Whyman, *Journal of the chemical society-chemical communications*, 1994, **72**, 801-802.
24 I. Hussain, S. Graham, Z. Wang, B. Tan, D. C. Sherrington, S. P. Rannard, A. I. Cooper and M. Brust, *J. Am. Chem. Soc.*, 2005, **127**, 16398-16399.
25 Y. Negishi and T. Tsukuda, *J. Am. Chem. Soc.*, 2003, **125**, 4046-4047.
26 J. Niu, T. Zhu and Z. Liu, *Nanotechnology*, 2007, **18**, 325607.
27 W. Halss, N. T. K. Thanh, J. Aveyard and D. G. Femig, *Anal. Chem.*, 2007, **79**, 4215-4221.
28 E. Sadauskas, G. Danscher, M. Stoltenberg, U. Vogel, A. Larsen and H. Wallin, *Nanomedicine : nanotechnology, biology, and medicine*, 2009, **5**, 162-169.
29 S. K. Balasubramanian, J. Jittiwat, J. Manikandan, C. N. Ong, L. E. Yu and W. Y. Ong, *Biomaterials*, 2010, **31**, 2034-2042.

Metabolizable dopamine-coated gold nanoparticles aggregates: Preparation, characteristics, computed tomography imaging, acute toxicity, and metabolism *in vivo*

Yao Yu, Youshen Wu, Jiajun Liu, Ke Li, Daocheng Wu*

The Key Laboratory of Biomedical Information Engineering of Ministry of Education, School of Life Science & Technology, Xi'an Jiaotong University, Xi'an, 710049, P.R.China

We prepared metabolizable MSA AuNPs@DPA aggregates, which exhibit improved CT imaging results, much lower toxicity and much longer circulation time *in vivo*.